DISTRIBUTION STATEMENT A. Approved for public release; distribution is unlimited.

New Approaches to the Parameterization of Gravity-Wave and Flow-Blocking Drag due to Unresolved Mesoscale Orography Guided by Mesoscale Model Predictability Research

Stephen D. Eckermann
Geospace Science & Technology Branch
Code 7631, Space Science Division
Naval Research Laboratory
Washington, DC 20375
Phone: (202) 404-1299 Fax: (202) 404-7997 email: stephen.eckermann@nrl.navy.mil

Award Number: N0001411WX21220
http://www.nrl.navy.mil/ssd/

LONG-TERM GOALS

When surface flow impinges on orography with horizontal scales of ~1-500 km, a variety of mesoscale dynamical responses can result, including gravity waves, upstream blocking, flow splitting and lee vortices. These dynamics produce important drag forces on the larger scale atmosphere. Because global numerical weather and climate prediction (NWCP) models under-resolve orography at these scales, all credible NWCP systems must include parameterizations of these missing orographic mesoscale drag (OMD) forces. Recent evidence from mesoscale model simulations clearly indicates that OMD forces cannot be described as a purely deterministic response to upstream forcing, but instead can exhibit a range of values, time histories and states. Our long-term goals are (a) to build these new OMD dynamics delineated from mesoscale models into a new class of OMD parameterizations, (b) to embed those new parameterizations within Navy NWCP systems, and (c) to investigate whether improved time-mean OMD and new explicit OMD variability can improve NCWP skill in Navy global NWCP systems across a range of scales.

OBJECTIVES

The objective of this project is to develop a new unified class of subgrid-scale parameterizations of gravity-wave and flow-blocking drag due to flow incident upon unresolved mesoscale orography that (a) builds upon the existing OMD parameterization currently implemented in Navy NWCP models (Webster et al. 2003), but (b) modifies it's behavior in ways that both recognize and explicitly incorporate realistic distributions of possible OMD values that can arise for a given upstream flow environment, as deduced from fully nonlinear mesoscale model ensemble simulations.

APPROACH

Our approach involves a three-tiered research, development and transition (RD&T) strategy based around (a) first-principles mesoscale modeling of the fundamental nature and morphology of OMD dynamics, (b) OMD parameterization based on the results from (a), and (c) objective testing of these new OMD parameterizations in Navy NWCP models.

For tasks in (a) we leverage results from detailed suites of high-resolution simulations of orographic mesoscale flow dynamics from the Coupled Ocean-Atmosphere Mesoscale Prediction System (COAMPS®), both those from larger research projects at the Naval Research Laboratory (NRL) and a specific subset of companion simulations in this project specifically targeted to our OMD objectives. We analyze these mesoscale model fields to characterize the properties of OMD in various flow and orographic environments (both idealized and realistic). The resulting statistics are compiled as a function of time, mountain height (inverse surface Froude number) and obstacle aspect ratio, using the "regime diagram" approach that currently defines deterministic OMD responses in parameterizations (see Figure 1). This work delineates regions of this regime space that yield reproducible (deterministic) OMD and others that instead yield vacillating or even chaotic OMD. These new results in turn facilitate generalizations of the deterministic regime diagram responses in current OMD parameterizations to new hybrid responses that can vary, from constant deterministic OMD, to periodic/vacillating OMD, to purely stochastic and/or chaotic OMD, depending on their location in the regime space of Figure 1.

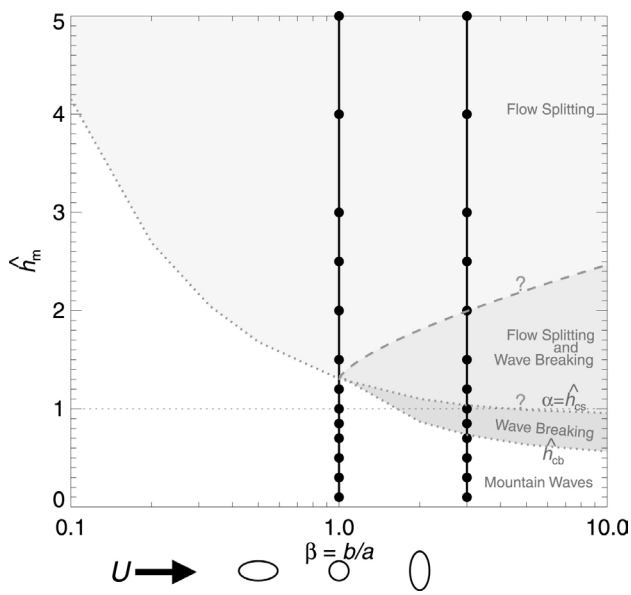

Figure 1. Regime diagram delineating OMD responses to uniform upstream flow of speed U and stability N, as a function of normalized obstacle height $\hat{h}_m = h_m N / U$ ***and obstacle aspect ratio β (after Eckermann et al. 2010).***

Tasks in category (b) focus on modifying the existing deterministic OMD scheme of Webster et al. (2003) in the Navy Global Environmental Model (NAVGEM) to include more realistic OMD properties and variability. Based on the existing literature (e.g., Doyle and Reynolds 2008; Eckermann et al. 2010), there appear to be (at least) two types of temporal OMD variability: (i) periodic vacillations due to cyclical buildup and breakdown of wavebreaking states, and (ii) quasi-chaotic vacillations due to complex internal sensitivities in the nonlinear mesoscale dynamics. We seek initial parameterizations of both types of response using explicitly stochastic methods, in which the range of temporal OMD variability is prescribed but the time history is random, thereby yielding realistic spread and variability in the time mean. For the orographic gravity-wave (OGW) component, we pursue the stochastic approach developed for multi-wave nonorographic gravity-wave drag (NGWD) by Eckermann (2011), and apply it to the orographic problem. Since multiwave methods are required for accurate OGWD parameterization in three-dimensional flows across three-dimensional obstacles

(e.g., Shutts 1995), we seek single-wave stochastic analogues for those applications based on the successful NGWD approach of Eckermann (2011). We also seek to use powerful new Hilbert transform methods based on the diagnostic Fourier-ray method described by Eckermann et al. (2010) for analyzing the gravity-wave content of mesoscale model output. In particular, we apply the method to quantify and parameterize for the first time the important process of three-dimensional geometrical spreading and its effects on wave amplitude growth with height and the transition to wave breaking and drag, a process currently omitted entirely from parameterizations. Since the total OMD across the obstacle must also be apportioned into OGW and orographic flow-blocking (OFB) contributions, we also seek stochastic parameterizations for the surface OFB component, based on (a) extending the simple analytical current calculations based on critical Froude numbers that locate the altitude of a dividing streamline, and (b) adapting the Webster et al. (2003) approach of heuristic fits to model-simulated OFB to incorporate realistic ranges of modeled variability within stochastic frameworks.

Tasks in category (c) implement the new OMD parameterizations in NAVGEM and assess performance, first in offline single column tests and ultimately in full forecast-assimilation experiments with results benchmarked using objective skill scores.

WORK COMPLETED

The following tasks were performed in this third year of work, building upon work completed in Years 1 and 2 and documented in our reports from previous years.

- We implemented in NAVGEM the first version of our unified gravity-wave drag parameterizations based on the accumulated research results from this project (see Figures 4 and 5);
- We tested the scheme in NAVGEM using long-term forecasts and full forecast-assimilation runs, which revealed statistically significant positive impacts at upper altitudes (see Figures 6 and 7);
- We implemented and tested initial versions of the geometrical spreading influence on wave amplitude evolution with height and the transition to instability and wave breaking, based on new simplified lookup table fits capturing results from our ray-based studies of this effect across the gravity-wave parameter space defined by altitude (z), obstacle aspect ratio (β) and obstacle orientation angle to the flow (α), as documented here and in previous reports (see Figures 2 and 3).
- We implemented initial regime diagram responses in the parameterized OMD based on collated COAMPS, and ray experiments as well as consensus findings from the literature (see Figure 5).

RESULTS

Parameterization of Geometrical Spreading Throughout the Parameter Space

a. Sensitivity to Obstacle Shape

Previous reports have documented in detail our research aimed at capturing the important, but never-before parameterized, effect of geometrical spreading on the evolution of wave amplitudes with height and the transition to threshold amplitudes for wave breaking and momentum deposition resulting in drag forces on the model's resolved flow. In particular, this work has focused on defining the dominant

dependences throughout the wave parameter space defined in part by Figure 1, and specifically as a function of altitude (z), obstacle aspect ratio (β), obstacle orientation angle to the flow (α), and obstacle shape.

An important finding to come out of this year's research was a remarkable insensitivity of this geometrical spreading to details of the obstacle's three-dimensional shape. An example is shown in Figure 2, which profiles on the right the variation of normalized wave amplitudes with height due to geometrical spreading of the wave fields for various constant wind speeds. The collection of different wave amplitude curves on the right are computed for a range of different axisymmetric three-dimensional obstacle shapes, whose two dimensional cross sections are profiled in the left panel. This encompasses a broad range of obstacle shapes, ranging from sharp discontinuous "pointy" topography like the cone shape, to smoothly varying broader obstacles like the Witch of Agnesi profiles. The corresponding geometrical spreading profiles on the right show almost no sensitivity to these comparatively large variations in the harmonic content of the parent obstacle.

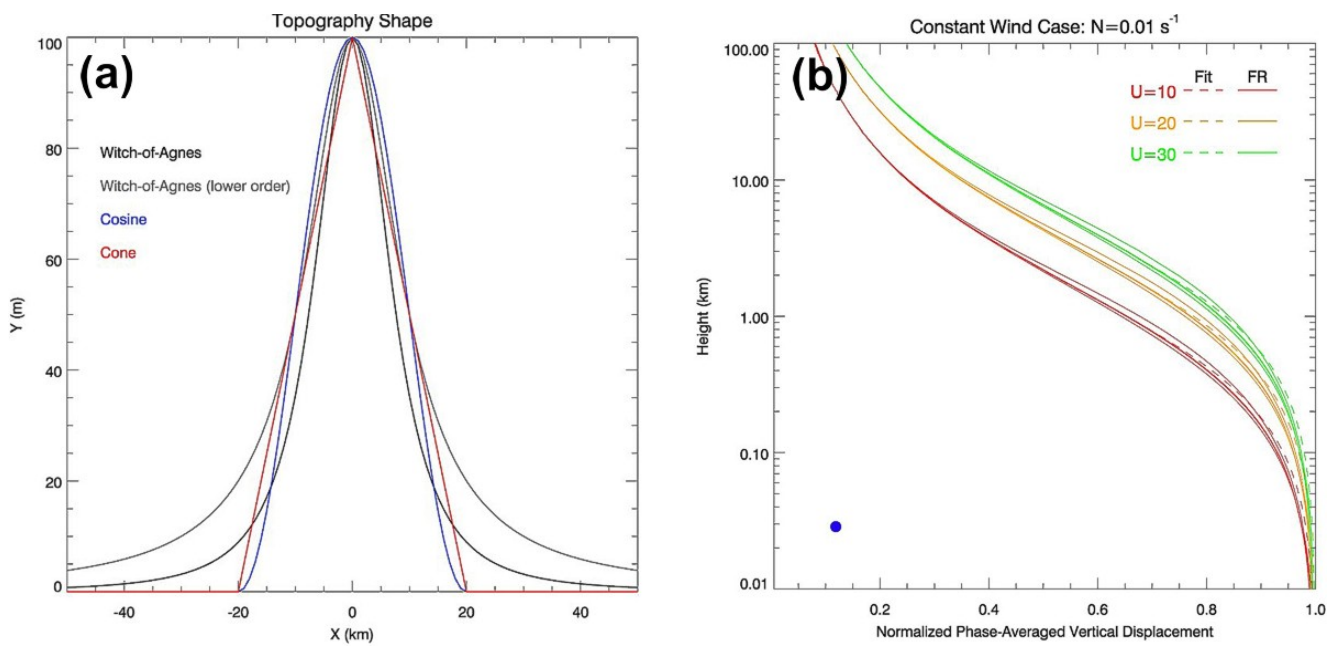

Figure 2. (a) series of different three-dimensional obstacle shapes, including two versions of the classical "Witch of Agnesi" shape (black and gray), a truncated cosine function (blue) and a triangular cone function (red). The normalized geometrical spreading with height of the resulting three-dimensional wave fields for each obstacle shape are depicted on the right for wind speeds U of 10 m s^{-1} , 20 m s^{-1} and 30 m s^{-1}, and all cluster tightly around the same profile shape for a given U, despite the differences in obstacle shape. See text for further details.

This is an entirely new finding, and is a powerful result for parameterization. Since subgridscale orography has complex and variable spatial content, any strong dependence of geometrical spreading on the shape details of the three-dimensional subgrid-scale orography would present considerable challenges to parameterizations. Results like those in Figure 2 indicate that this geometrical spreading is remarkably insensitive to these details, a property that considerably simplifies the parameterization of these effects in NAVGEM.

b. Sensitivity of Obstacle's Orientation with respect to the Surface Flow Direction

Previous work has mapped out the geometrical spreading within a two-dimensional parameter space defined by altitude *z* and the obstacle's ellipitical axial ratio β. There is however a third dimension of relevance for parameterization, which encapsulates gravity-wave responses and geometrical spreading rates when the elliptical obstacle is aligned at various angles α to the surface flow U. In essence, this represents a semicircular axis that connects the responses for obstacles of axial ratio β and 1/β, as is depicted by the colored obstacle progressions shown just above the abscissae of Figure 3.

The points and curves in Figure 3 map out geometrical spreading results and analytical fits, respectively, derived from FR experiments for an elliptical obstacle of β=3 (black obstacle) as it is successively rotated with respect to the mean flow direction until it reaches the β=1/3 limit (yellow obstacle). The resulting geomretical spreading curves for different mean flow speeds *U* are shown. Again, there is a smooth and reproducible variation in the geometrical spreading curves between the limiting curves at β=3 and β=1/3 as α is varied. We have experimented with various fitting algorithms to capture this third dimension of geometrical spreading variability for parameterization, currently favoring a working fit based on fits as a function of log β, since this variable is both linear and symmetric about β=1 and enables a simpler connection to the α dependences above. Closer fits to all these curves are still being sought across the entire (z,β,α) parameter space, but the working fits we have for now are close enough to enable first-order geometrical spreading effects to be incorporated into the paramaterizations for the first time.

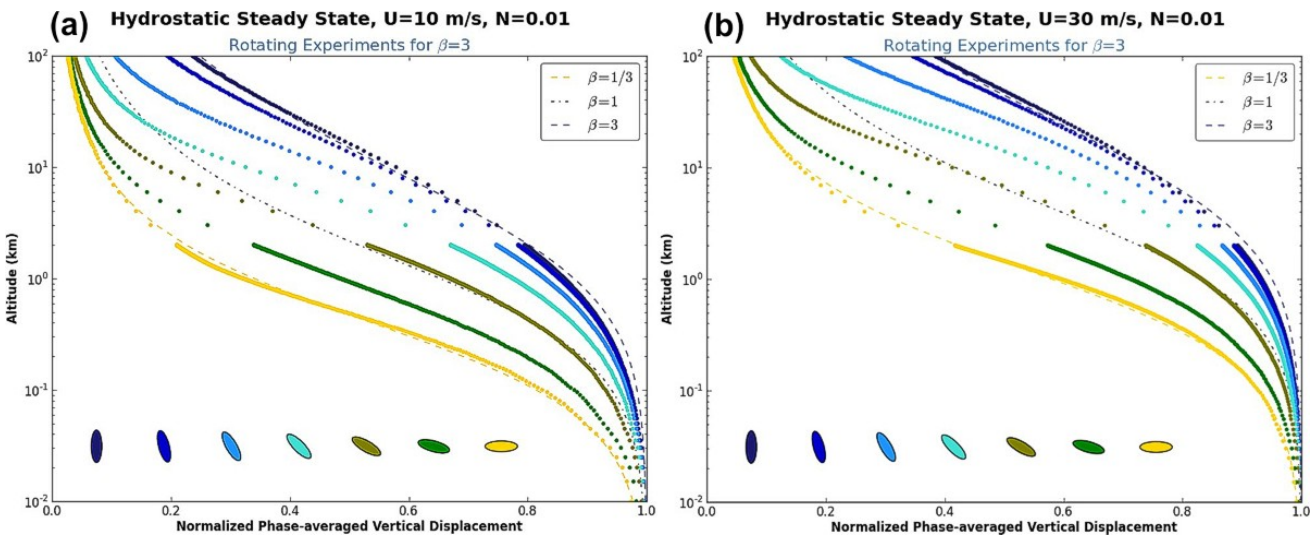

Figure 3. Variation with height of normalized peak wave vertical displacement amplitude, which varies due to geometrical spreading of three-dimensional wave fields, as an elliptical obstacle of β=3 is progressively rotated (as shown by obstacles depicted and colored at the base of each plot) through a range of azimuth angles α with respect to the mean flow direction (always from left to right). Results are shown for (a) U=10 m s^{-1} and (b) U = 30 m s^{-1}.

This new research work on geometrical spreading effects on wave amplitudes, which as demonstrated below is now feeding into the parameterizations for NAVGEM, is now largely complete and so is currently being written up for publication in the peer-reviewed literature (Eckermann et al. 2013).

Inaugural Unified NAVGEM Gravity-Wave Drag Parameterization

This year we finalized and implemented the inaugural version of our unified parameterization of subgrid-scale gravity-wave drag for use in NAVGEM, based on our research to date.

As illustrated in Figure 4, there are four nominal sources of subgrid-scale gravity-wave momentum flux and drag considered relevant for parameterization in models: (a) flow over subgrid-scale orography; (b) deep subgrid-scale convective forcing; (c) subgrid-scale dynamical flow imbalances due to underresolved jet or frontogenesis zones, and (d) all other indistinct and sporadic sources of gravity waves that give rise to a characteristic background spectrum of wave energy (see, e.g., Fritts and Alexander 2003). Figure 4a depicts how all four of these sources of subgrid-scale gravity-wave drag are separately parameterized currently in models.

Figure 4b, by contrast, illustrates our initial unified gravity-wave drag parameterization developed for NAVGEM this year based on the accumulated research to date in this project. Most notably, the physical routines governing wave propagation and amplitude evolution throughout the atmosphere, and the transition of wave amplitudes to thresholds for instability and wave breaking, are now parameterized by a common unified code, which accepts as inputs parameterized gravity waves from all four potential sources. In our initial implementation of this scheme, we are only parameterizing two of these wave sources, namely orographic gravity waves (the major focus of this particular project) and the background spectrum of wave activity. Currently, as depicted by the gray shading in Figure 4b, we are not receiving inputs from waves generated by subgrid-scale convection or jet instabilities. However, the code has been developed in a sufficiently generalized way that, when these parameterizations become available through future research, they will slot easily and seamlessly into this unified parameterization code at the locations indicated in Figure 4b.

Also evident in Figure 4b are significant augmentations and improvements to the physics of our unified parameterizations of wave propagation and wave breaking. These upgrades now include the generation of turbulence by wave breaking and the subsequent effect this wave-induced turbulence has on the model's resolved dynamics through the turbulent mixing of momentum, heat and constituents. Likewise, wave breaking also results in a frictional dissipation of wave kinetic energy that produces dynamical heating. This heating effect is tiny in the lower atmosphere and so has traditionally never been parameterized. However, the contribution from this term becomes significant at upper levels. More generally, however, it is critical to include both the turbulent and frictional wave heating contributions at all levels in order to maintain a strict and mutually consistent conservation of energy and momentum as these quantities are exchanged between the parameterization and the model's resolved dynamics, which is clearly a critical prerequisite for accurate predictions.

The detailed new results (documented above and in previous year's reports) pertinent to the orographic gravity wave and flow blocking responses at the source in Figure 4b have also been built into this new scheme in preliminary and simple ways that facilitate easier initial testing and tuning in NAVGEM. These new reponses are summarized in Figure 5 in terms of the regime diagram of Figure 1.

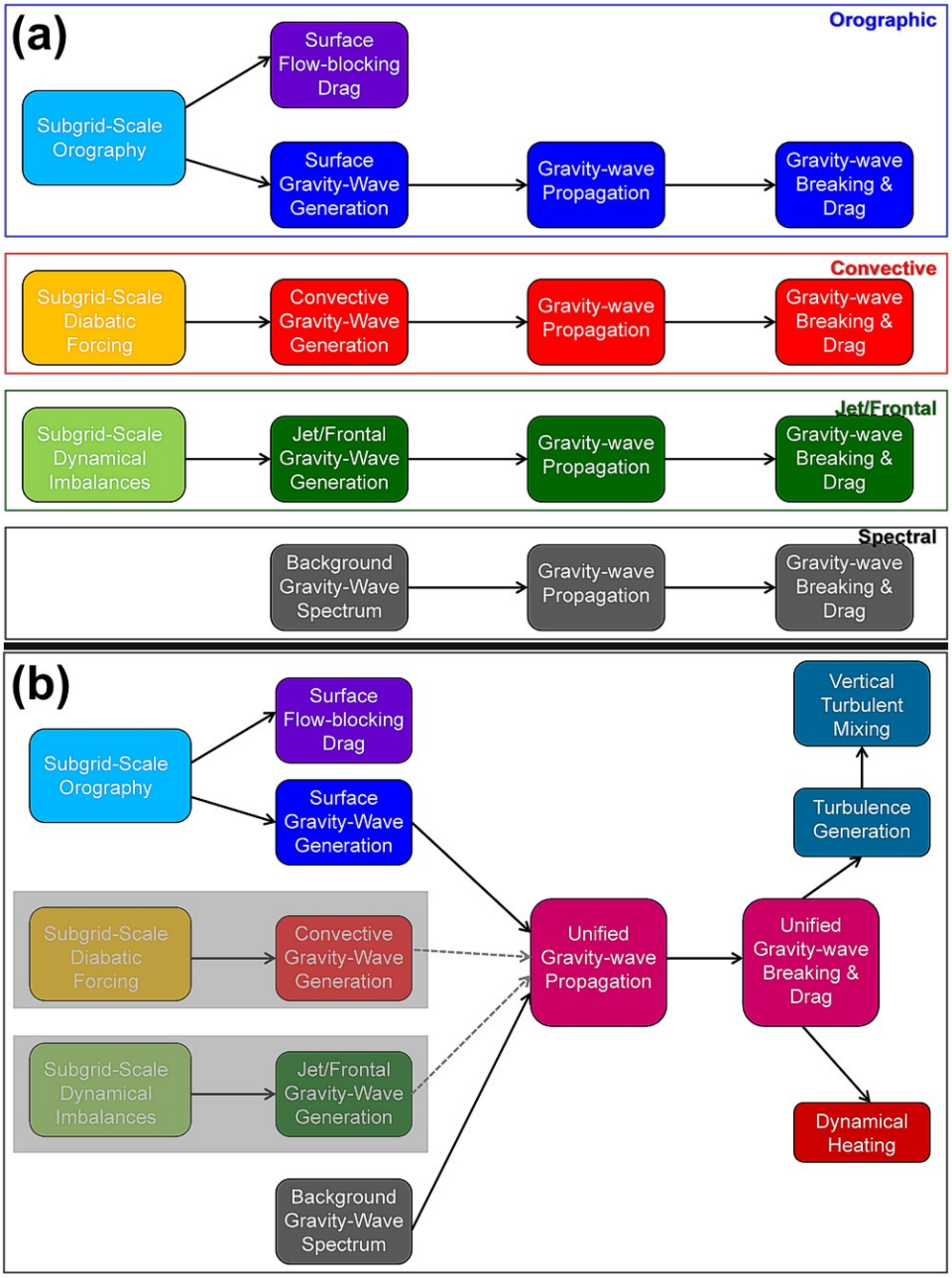

Figure 4. Flow diagram of the initial unification of physical mechanisms within the inaugural NAVGEM gravity-wave drag code. Panel (a) shows the current separate parameterizations of gravity-wave drag due to flow across subgrid-scale orography (blue), deep subgridscale convection (red), jet/frontal instabilities (green), and indistinct wave sources producing a background spectrum of waves (gray). Panel (b) shows the unification of the wave propagation and breaking components into a common code which accepts inputs from all wave sources. Note also the additional physics of turbulence generation and mixing, and dynamical wave heating. See text for further details.

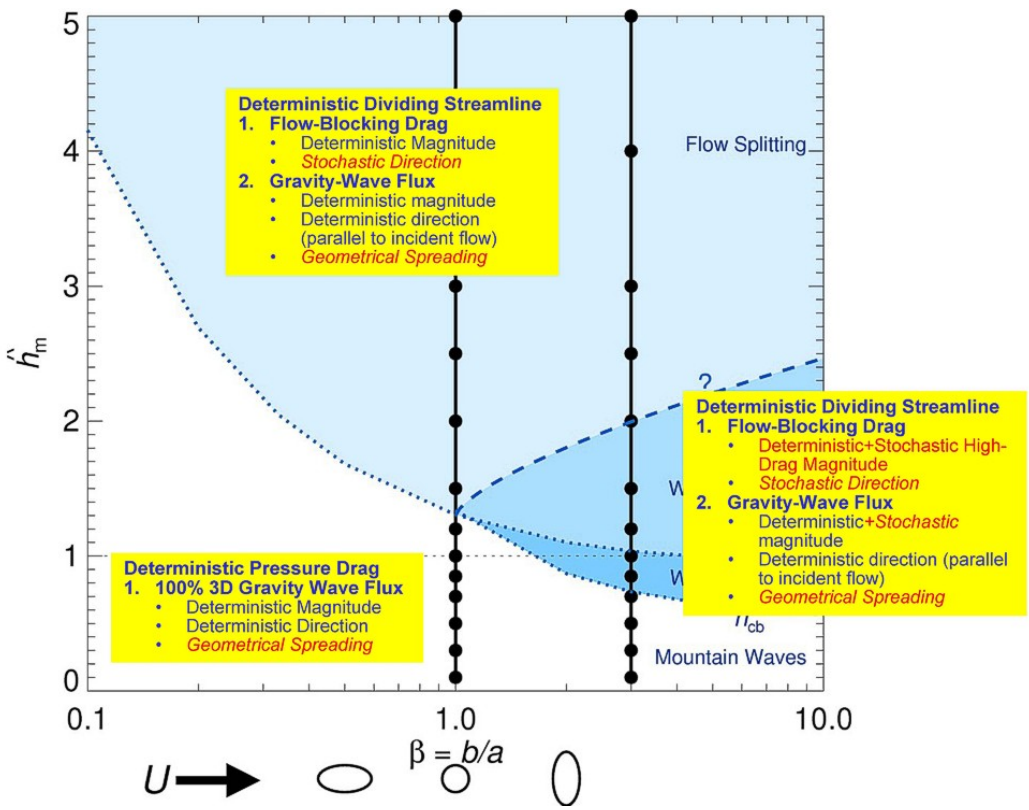

Figure 5. Red text summarizes the new features of the orographic gravity-wave and flow-blocking source dynamics implemented into the new gravity-wave drag parameterization in Figure 4b, summarized according to the flow response within the regime diagram of Figure 1.

As outlined next, this scheme has been extensively tested this year, first in the NAVGEM single column model, then in long forecasts with the NAVGEM semi-Lagrangian (SL) forecast model, and finally using the full NAVGEM system (forecast model and data assimilation system) in long-term forecast-assimilation update cycle runs. The code is in the process of being fully integrated into the NAVGEM development branch under subversion revision control, where it will be available for use to the entire NAVGEM community at the Naval Research Laboratory. We anticipate this initial integration into the development branch to be completed by the end of October.

Initial Performance in NAVGEM

The unified parameterization has had immediate positive impacts in NAVGEM, despite little time to date for tuning and baselining of the new scheme.

Figure 6 shows an example of the positive impacts. The blue curves show mean analyzed temperatures averaged from 60°-80°N from a control NAVGEM T359L60 run without the new parameterized gravity-wave drag. The actual temperatures observed at this time and altitude are plotted in red, and were derived from independent research observations from the Microwave Limb Sounder (MLS) on NASA's Aura satellite. The blue and red curves reveal a substantial cold bias in the analyzed NAVGEM stratospheric temperatures in boreal winter, when the Sun disappears at high latitudes and

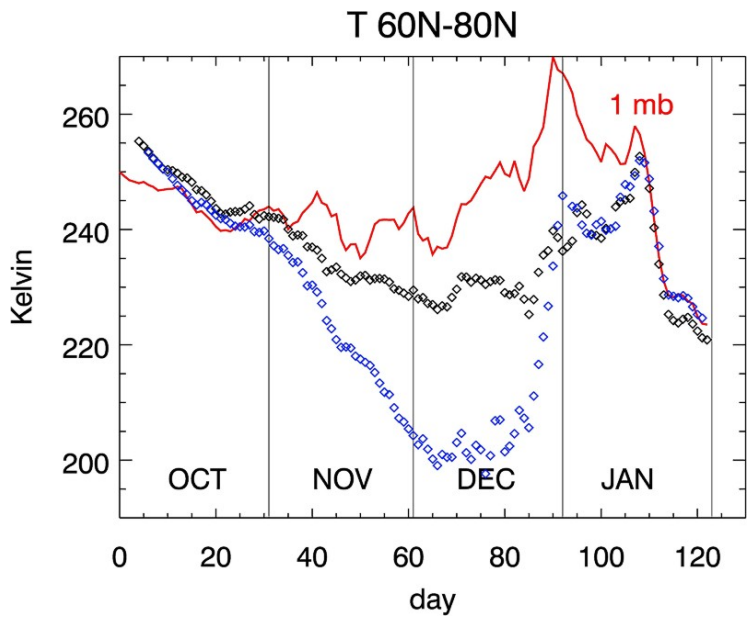

Figure 6. Time series of analyzed NAVGEM temperatures (K) versus time (1 October 2011 to 10 February 2012) at 1 hPa (~48 km altitude) for a control run (blue symbols) and a run including the new unified gravity-wave drag scheme (black symbols). Observed temperatures from the Microwave Limb Sounder on NASA's Aura satellite are plotted in red.

the region receives no incoming solar radiation to directly heat the atmosphere. The reason why observed MLS temperatures are warm is due to a gravity-wave-drag-driven circulation that produces a mean poleward and downwelling circulation cell that adiabatically warms the stratosphere.

The black curves in Figure 6 show the results from a corresponding T359L60 NAVGEM run which included the new unified gravity wave drag parameterization depicted in Figure 4b. It should be noted that a complete test of this scheme in NAVGEM requires careful tuning of the wave source parameters to get a reasonable long-term climate, whereas this test was performed using the default "out of the box" settings. Despite this, the NAVGEM run with gravity-wave drag (black curve in Figure 6) produces a substantially improved 1 hPa temperature analysis relative to the control (blue curve) that immediately and substantially improves the cold bias with respect to the independent MLS Aura observations (red curve). It is clear that the scheme is already having immediate large positive impacts on NAVGEM prediction skill in the upper stratosphere.

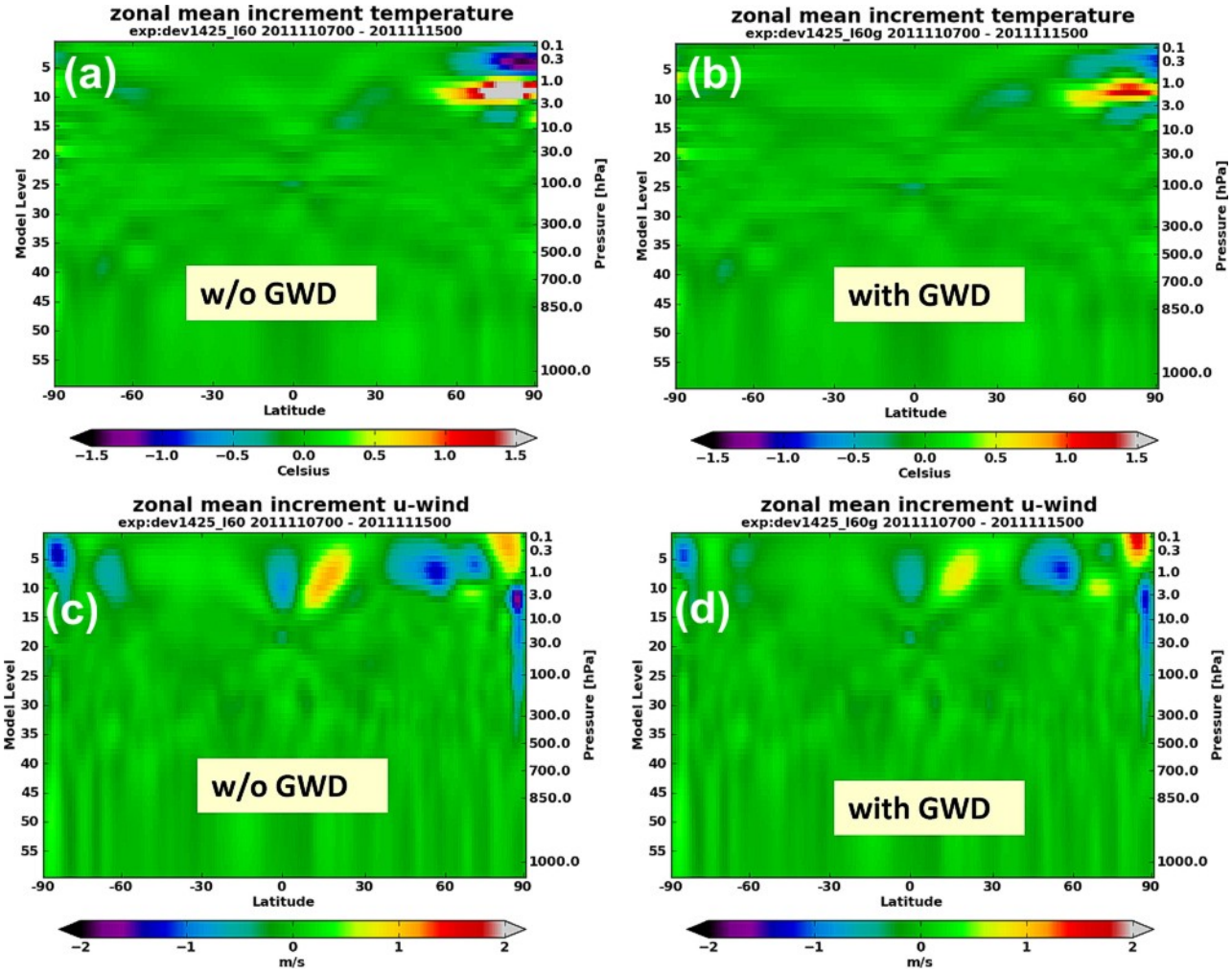

Figure 7. Zonal-mean temperature increments versus NAVGEM model level (left axis, pressure on right axis) and latitude averaged over 7-15 November 2011 for T359L60 NAVGEM update cycle experiments. Results as shown for temperature (top row) and zonal winds (bottom row) for a control experiment without gravity-wave drag (left) and a corresponding experiment that includes the new unified gravity-wave drag parameterization (right), which reduces observational increments everywhere relative to the control.

Figure 7 shows objective scores based on zonal mean temperature and zonal-wind increment statistics, averaged for the period 7-15 November 2011. The increments are the observational corrections to the forecast model applied during the data assimilation phase, and generally indicate forecast biases. The panels on the left show temperature and zonal wind increments from the control NAVGEM run without the new gravity-wave drag drag. The corresponding results on the right come from the NAVGEM run with the new gravity-wave drag parameterization included, and show substantial reductions in both upper-level temperature and zonal wind increments, both at high latitudes and in the tropics.

IMPACT/APPLICATIONS

The results presented above illustrate that the new research results that have fed into a new unified gravity-wave drag parameterization for NAVGEM (Figure 4b) are having immediate and major beneficial impacts on NAVGEM at upper levels by reducing temperature and zonal wind biases (Figures 6 and 7). These results are appearing despite no tuning of these schemes to improve the model climate to date, and so results this positive so early in the parameterization development cycle are extremely encouraging in terms of improving NAVGEM skill in the stratosphere, with flow on effects at all levels through improved deep circulations and data assimilation.

TRANSITIONS

The new unified gravity-wave drag parameterization is in the last stages of a full transition into the NAVGEM development branch, at which point it will become fully available for use by all NRL researchers and developers of the NAVGEM code. Pre-operational testing of the scheme for future FNMOC transitions are planned in the next 6-12 month timeframe.

RELATED PROJECTS

Doyle, J. D., and S. D. Eckermann, *The Boundary Paradox*, NRL 6.1 Accelerated Research Initiative, 1 October 2010-30 September 2015.

REFERENCES

Doyle, J. D. and C. A. Reynolds (2008), Implications of regime transitions for mountain-wave-breaking predictability. Mon. Wea. Rev., 136, 5211–5223.

Eckermann, S. D. (2011), Explicitly stochastic parameterization of nonorographic gravity-wave drag, J. Atmos. Sci., 68, 1749-1765.

Eckermann, S. D., J. Lindeman, D. Broutman, J. Ma and Z. Boybeyi (2010), Momentum fluxes of gravity waves generated by variable Froude number flow over three-dimensional obstacles, J. Atmos. Sci., 67, 2260-2278.

Fritts, D. C., and M. J. Alexander (2003), Gravity wave dynamics and effects in the middle atmosphere. Rev. Geophys. 41, doi:10.1029/2001RG000106.

Shutts, G.J. (1995), Gravity-wave drag parametrization over complex terrain: The effect of critical-level absorption in directional wind-shear. Quart. J. Roy. Meteor. Soc., 121, 1005-1021.

Webster, S., A. R. Brown, D. R. Cameron, and C. P. Jones (2003), Improvements to the representation of orography in the Met Office Unified Model. Quart. J. Roy. Meteor. Soc., 129, 1989–2010.

PUBLICATIONS

Broutman, D., and S. D. Eckermann (2012), Analysis of a ray-tracing model for gravity waves generated by tropospheric convection, J. Geophys. Res., 117, D05132, doi:10.1029/2011JD016975.

Eckermann, S. D. (2011), Explicitly stochastic parameterization of nonorographic gravity-wave drag, J. Atmos. Sci., 68, 1749-1765.

Eckermann, S. D., J. Ma, and D. Broutman (2013), Geometrical spreading and the parameterization of orographic gravity-wave drag, J. Atmos. Sci. (paper in preparation).

HONORS/AWARDS/PRIZES

1. Stephen Eckermann was awarded the 2013 Sigma-Xi Award for Applied Science from the NRL Edison Chapter for foundational contributions to the Navy's high-altitude forecasting and analysis capabilities
2. Stephen Eckermann was awarded the 2013 American Meteorological Society's Editor's Award of the Journal of the Atmospheric Sciences for "thorough and detailed reviews with well-informed, well-posed and carefully argued questions for authors": see http://www.ametsoc.org/awards/2013awardrecipients.pdf
3. Stephen Eckermann was one of ten NRL awardees of the Navy Acquisition Excellence Award for Technology Transition, for the Navy Global Environmental Model (NAVGEM): see http://www.nrl.navy.mil/media/news-releases/2013/nrl-receives-navy-acquisition-excellence-award-for-global-weather-prediction-model